AIMS Energy, 13(1): 125–146.
DOI: 10.3934/energy.2025005
Received: 29 October 2024
Revised: 22 January 2025
Accepted: 11 February 2025
Published: 18 February 2025

http://www.aimspress.com/journal/energy

Research article

Forecasting of energy consumption rate and battery stress under real-world traffic conditions using ANN model with different learning algorithms

Anbazhagan Geetha[1], S. Usha[1], J. Santhakumar[2] and Surender Reddy Salkuti[3,*]

[1] Department of Electrical and Electronics Engineering, College of Engineering and Technology, Faculty of Engineering and Technology, SRM Institute of Science and Technology, Kattankulathur, Chengalpattu, Tamil Nadu 603203, India
[2] Department of Mechanical Engineering, College of Engineering and Technology, Faculty of Engineering and Technology, SRM Institute of Science and Technology, Kattankulathur, Chengalpattu, Tamil Nadu 603203, India
[3] Department of Railroad and Electrical Engineering, Woosong University, Daejeon 34606, Republic of Korea

* **Correspondence:** Email: surender@wsu.ac.kr; Tel: +821096741985.

Abstract: Estimating energy consumption rates is a necessary step when building infrastructure for charging and schedule optimization of battery-powered vehicles utilized in public urban driving patterns. This study examined several input factors for the prediction of vehicle performance. Input conditions were energy management controls, State of Charge (SOC) power train batteries, and ultra-capacitor vehicle models; output metrics included consumption rates, battery loads, and trip distances. To examine the experimental design, an L9 design was used with four control factors at three different levels each. Artificial neural network (ANN) models were developed employing four learning algorithms: quick propagation (QuP), batch backpropagation (BBaP), Levenberg-Marquardt backpropagation (LMBaP), and incremental backpropagation (IBaP). Post-simulation results were summarized and validated using the root mean square error (RMSE), which indicated that the values collected experimentally were close to those predicted by the models. This paper built an ANN-based prediction model and accurately predicted vehicle performance and potential energy shortfalls in public transportation networks. These insights can be applied to interventions like charging stations or reshaping bus timings to avoid power loss.

Keywords: Hybrid electric vehicle; energy management control strategies; artificial neural network; learning algorithm; LM backpropagation algorithm

1. Introduction

The advent of electric vehicles (EVs) promises a profound transformation in human existence. By 2024 it is predicted that there will be over 40 million electric vehicle owners. The number of EVs generated annually is increasing; according to OICA data, approximately 90 million EVs were produced in 2015. Still, vehicles using internal combustion engines (ICEs) are at the top of the current social hierarchy, being the biggest source of greenhouse gas emissions. Roadways cause approximately 90% of carbon monoxide, 40% of nitrogen oxide, and 25% of carbon dioxide emissions [1,2]. Human health is significantly harmed by atmospheric air pollution. According to WHO data, air pollution caused over 7 million deaths worldwide by the year 2012. Current concerns over the state of the atmosphere, specifically greenhouse gas emissions, have driven automobile manufacturers to refocus their efforts on electric vehicles. Data on worldwide sales and changes to electric cars from 2014 to 2024 is shown in Figure 1 [3].

The restricted power and energy storage system capacities of EVs are the main causes of their shorter driving ranges and subpar performance. The last few decades have seen an increased interest in vehicle electrification due to global environmental concerns and the inefficiency of ICE-based transportation. The United States Department of Energy Vehicles (EV) recently launched a funding effort to support developing battery technology, new large-scale power semiconductor devices, and power electronic technologies. More chances are expected for electrified transportation. Over the past few years, those opportunities have contributed to reducing the cost of EV energy storage systems (ESSs) to half their original cost [4]. In addition to lowering the price of batteries, other aspects such as their capability to handle energy and power and endurance also need to be improved. This could further guarantee the global development of EVs [5,6].

EVs are superior to traditional ICE vehicles in many ways. First, EVs are considerably more energy-efficient than other vehicles. In EVs, approximately 62% of the battery energy can be used to drive the vehicle wheel, compared to approximately 21% of gasoline energy that can be turned into useful driven power [7,8]. EVs are therefore green, eco-friendly, and clean. There are no greenhouse gas emissions from the exhaust of an electric vehicle. EVs use electrical motors; therefore, they are supposed to be quiet and smooth while traveling. Finally, compared to ICEs, they require less upkeep and repairs [9]. The tricky aspect of hybridization is managing the energy between the sources [10]. The mechanism that determines how much energy each ESS will share is called the energy management control strategy (EMCS) [11]. The vehicle's travel range is the primary factor, according to customers' vision [12]. Increasing the battery capacity is necessary for longer trip ranges, which raises the system's cost [13]. An energy management system for hybrid electric buses (HEBs) based on battery health awareness was introduced and designed via a twin delayed deep deterministic policy gradient (TD3) deep-reinforcement learning algorithm. This work integrates naturalistic driving data to design a more realistic energy management strategy that utilizes feedback from real-world traffic and driving conditions—an improvement of traditional rule-based approaches. Real-world driving data is processed to make the model robust and applicable in dynamic urban transport scenarios. The results of this study indicate that advanced reinforcement learning methods hold significant promise for the

redesign of sustainable transportation systems, enabling scalable solutions for improving efficiency and reliability in hybrid and electric vehicle networks [14,15]. Therefore, researchers must focus on the vehicle's dynamics. For hybridization to be complex, the storage systems' current state of charge is also important. Therefore, designing an effective EMCS is necessary [16].

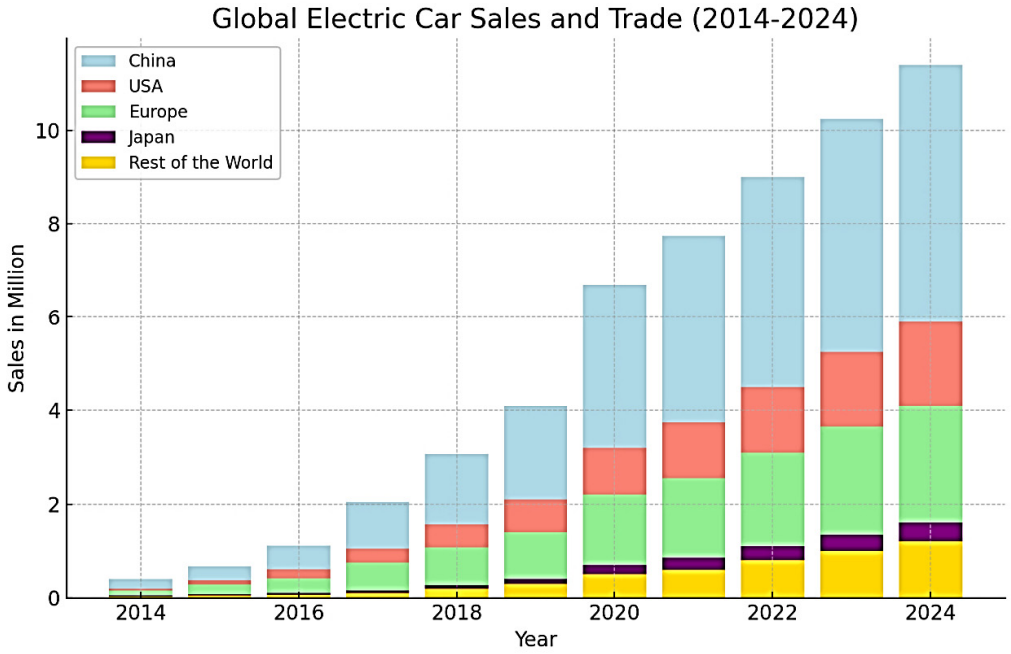

Figure 1. Global electric car sales and trade.

Artificial neural network-based control strategies for energy management between hybrid sources were developed by Moreno et al., who concluded that the traveling distance of test vehicles can be improved from 5.3% to 8.9% when using such strategies compared to other conventional control strategies [17,18]. Researchers evaluated unique hybridization based on the hydraulic concept, and the operating zone over which vehicles with DC motors and hydraulic motors may achieve maximum efficiency was determined using a traditional rule-based control technique [19]. Additionally, dynamic programming has been used to identify the best control trajectories between the two sources [20–22]. Technology that recognizes driving patterns and uses dynamic programming has been used to create drive cycle patterns. Additionally, a fuzzy-based control approach was used to determine the drive cycle or present driving conditions. To achieve the best possible energy sharing mode, a hierarchical energy management method has been used [23]. Advances in applying reinforcement learning to intelligent transportation systems have shown that the SAC algorithm can solve continuous and dynamic control. The results have important implications for the adoption of sustainable mobility and the improvement of the efficiency of possible future eco-driving systems [24].

A sliding mode-based control strategy has been proposed, with results showing that energy sources can respond better to fast transient operations. From the literature, no research work has been carried out to predict the performances of the vehicles considered [25]. In this context, this work aims to develop prediction models for analyzing the effect of controlling factors (EMCS, vehicle model,

and ESS's charge state) on vehicle performance, i.e., energy consumption rates (ECR) and battery stress. The prediction model is based on artificial neural networks (ANNs) [26]. ANNs are a promising modeling technique with the potential to predict responses with lower amounts of data and higher accuracy, inspired by the structural and working aspects of the human brain. The application of ANNs in prediction processes has increased recently [27].

Current vehicles have limited battery capacities, and efficient operation requires a method for scheduling charging stops during daily operations. The task becomes more difficult as the transportation network and operating conditions grow in size. The positioning of charging stations, charging hours in the transportation network, and vehicle journey itineraries may all be optimized using an exact energy consumption estimation tool. In the case of extremely fluctuating traffic circumstances or undulating roads, using constant consumption rates is erroneous and leads to challenges in accurately estimating energy usage. The models available for energy consumption in journey itineraries cover a broad spectrum of driving methodologies. Comprehensive kinematic models of automobiles, route-based energy consumption scenarios, and models combining driving style traits, environmental variables, and vehicle design-related elements are all available.

The study proposed here revolve around the design of an ANN prediction model to improve energy control and prediction of EVs equipped with HESS. This study aims to propose solutions to some challenges like limited battery capacities, EMCS, and energy consumption estimation to enhance vehicle performance indicators including ECR and battery stress. From the models developed, this study uses the best-performing ANN model that contains four learning algorithms: quick propagation (QuP), batch backpropagation (BBaP), Levenberg-Marquardt backpropagation (LMBaP), incremental backpropagation (IBaP), and results are validated using their root mean square error (RMSE). This study's outcomes hold key operational and infrastructural implications and can thus contribute to the development of sustainable transportation to address challenges in operating and managing EVs. By using ANN modeling for its predictive power, this research increases the operational effectiveness of EVs in many dimensions. By being able to accurately forecast energy consumption rates (ECR) and battery stress, the real-time optimization of energy usage can be achieved to minimize energy inefficiency and facilitate vehicle operation.

By predicting and managing energy demands, strategic interventions can be carried out more effectively, including cheaper installation of charging stations and dynamically scheduling charging stops. These efforts not only improve the accessibility and reliability of the EV charging networks but also improve the total efficiency of the transportation systems in fluctuating traffic and environmental conditions. ANN-based predictions can also be applied to tailor route plans according to energy availability to minimize unplanned vehicle downtimes. From an environmental angle, the findings of this study directly result in decreasing greenhouse gas (GHG) emissions by enhancing energy usage efficiency while reducing the need for fossil fuels. In addition, the reduced stress on EV batteries increases their lifespan, reducing the need for replacements and lessening the environmental burden of production and disposal.

Moreover, ANN-driven methodologies create a platform for the integration of smart energy management systems into upcoming EV infrastructure. Based on these systems, the transportation ecosystem can also be made adaptive and resilient through real-time traffic data, weather conditions, and energy price fluctuations. The findings of this research further support the role of green mobility in combating climate change and creating sustainable urban development by supporting global initiatives to reduce carbon footprints.

This novelty of the research stands out due to the consideration of real traffic scenarios, driving behaviors, and individual vehicle factors when developing the ANN model. It uses single performance metrics as one of the prediction targets, demonstrating high accuracy in predicting both ECR and battery stress, being implemented using a variety of learning techniques. Moreover, the presented LMBaP with optimized parameters is a new approach to minimizing prediction errors and can be effectively used in dynamic conditions of urban environments.

In this paper, section 2 deals with the experimental design and the selection of control factors. Section 3 elaborates the control strategy and driving cycle details. Section 4 describes and discusses the results of the proposed ANN prediction model. Section 5 concludes the analysis.

2. Experimental design and procedure

Figure 2 shows the vehicle configuration considered for the present work. A unidirectional boost converter between the DC bus and battery and a bidirectional buck-boost converter between the DC bus and UC was utilized. The vehicle has a Permanent Magnet DC (PMDC) motor. The two-way power converter is responsible for efficiently capturing power during braking.

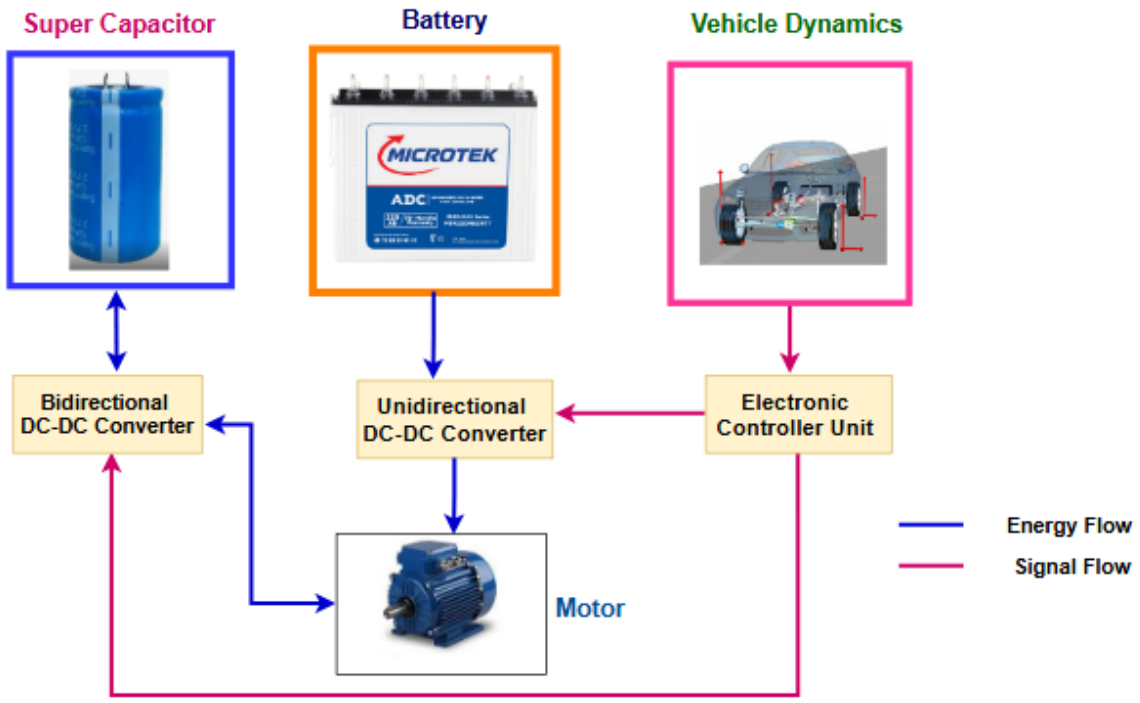

Figure 2. Proposed vehicle configuration.

2.1. Control factors

The vehicle's performance is highly influenced by major vehicle specification factors like the mass of the automobile, the air-drag coefficient, and the front area of the vehicle. The vehicle's mass relates to the vehicle without load, storage, or travelers. A_1, A_2, and A_3 represent varying levels of

electric vehicle specifications. All models were selected to ensure similar battery capacities. The vehicle models and their specifications are depicted in Figure 3.

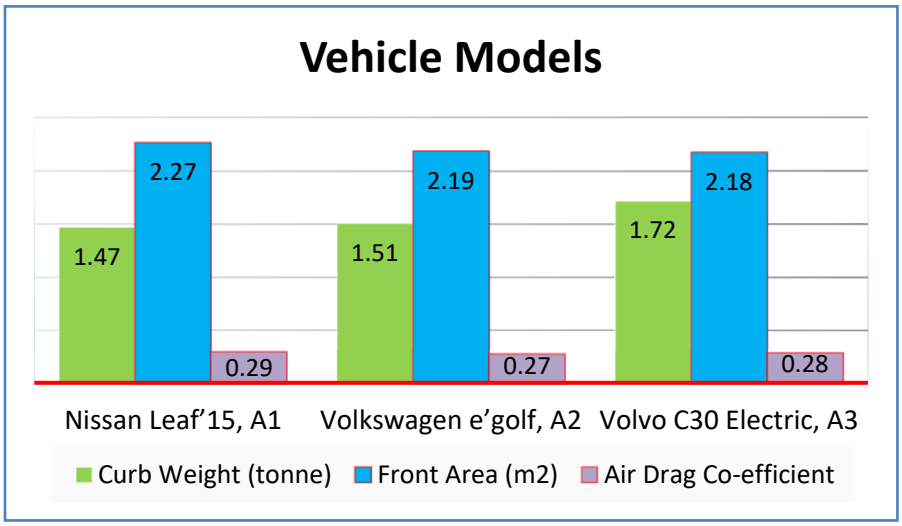

Figure 3. Specifications of the models under study.

The battery charge (SOC_{BAT}) levels are categorized as low, medium, and high. B1, B3, and B4 correspond to 40%, 60%, and 80% of SOC_{BAT}, respectively. The levels for the storage systems were chosen based on practical knowledge. The cut-off voltage of an ultra-capacitor is considered to be half its voltage. Hence, 50% (C1) is low, 75% (C2) is medium, and 100% (C3) is high. Table 1 denotes the levels of each controlling input factor selected for the study. For the 3 factors, each with 3 levels, either 9 or 27 experiments can be done. Here, 9 experiments were considered, since they allow the same effects of 27 experiments while reducing experimental time.

Table 1. Hybrid Electric Vehicle (HEV) controlling input factors with levels.

Control factors	Level 1	Level 2	Level 3
Vehicle model	A1	A2	A3
SOC_{BAT}	B1	B2	B3
SOC_{UC}	C1	C2	C3

2.2. Vehicle dynamics

According to the mechanics of the vehicle, the force ($F_{required}$) needed for it to run must be higher than the rolling resistance force (F_{rollin}), climbing force (F_{clb}), and aerodynamic dragging force (F_{dragin}), as stated in Eq (1).

$$F_{required} = F_{rollin} + F_{clb} + F_{dragin} \tag{1}$$

$$F_{rolling} = m_{vehicle} * g_{acceleration} * C_{rollin} \tag{2}$$

$$F_{c1b} = m_{vehicle} * g_{acceleration} * C_{rollin} \tag{3}$$

$$F_{dragin} = \frac{(\rho * A_{front} * C_{dragin} * v_{vehicle}^2)}{2} \tag{4}$$

The force (F_{rollin}) needed to overcome the friction losses from tires and the road is indicated in Eq (2). The vehicle's need to overcome topographical impacts (F_{clb}) is shown in Eq (3). The EV's (F_{dragin}) power to overcome air resistance on its back, front, and boundary sections is as shown in Eq (4).

Vehicle mass is given in kg, and $g_{acceleration}$ is the acceleration (m/s^2) caused by gravity. C_{rollin} represents the rolling resistance coefficient. The drag coefficient is given by C_{dragin} (kg/m^3) represented by the air density, and ρ A_{front} is the frontal area of the car (m^2). The vehicle's velocity is given in km/h.

2.3. Performance characteristics

Here, X_1 represents the energy consumption rate (ECR), and X_2 is the stress occurring in the battery. The respective mathematical equations are given in Eqs (5) and (6).

$$X_1 = \frac{Power_{consumed}}{Range_{travelled}} \tag{5}$$

$$X_2 = \int \frac{\left|i_{battery}^2\right|}{time} dt \tag{6}$$

3. Selection of driving cycle and control strategy

The roadway, traffic patterns, and driving habits of the users in a given location are all reflected in the driving cycle of that location. Each region will have its driving cycle, which will reflect the conditions of that region. Here, the experimental setup generated a driving cycle in real-world circumstances along a chosen route. All four driving modes were recorded as micro-trips for a given time, and the average of those micro-trips was used to create the most realistic driving cycle. The real-time driving pattern considered was a moderate urban driving pattern. Figure 4(a) and (b) illustrate the road map and the developed driving cycle. The total duration of the driving pattern is 600 seconds, at an average speed of 54.6 km/h, covering a distance of 6.9 km.

Figure 4(a). Road map.

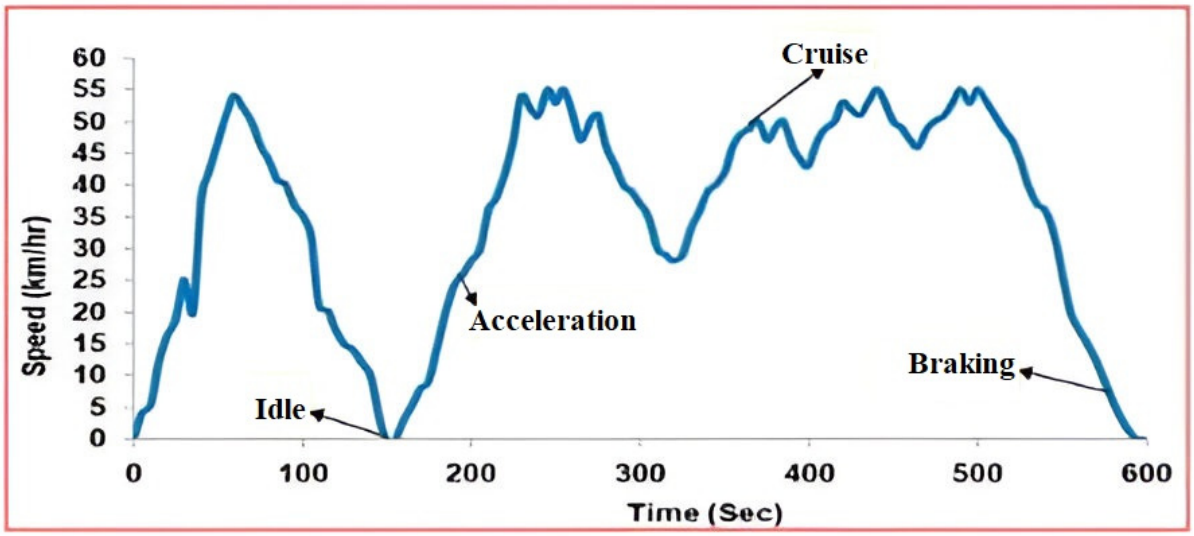

Figure 4(b). Real-time drive cycle.

Here, three control factors, each with three levels, were considered. As per the experimental design, the Taguchi L_9 (3^3) orthogonal array (OA) was implemented. The rule-based control (RBC) strategy was found to be an optimum control strategy for the multi-objective optimization explained in the literature. The flowchart for the RBC algorithm is given in Figure 5.

In RBC, the drive power required by the vehicle, found using vehicle dynamics, is divided into three categories: (i) Whenever the power demand is lower than or equal to the average power, the battery supplies the demand if SOC_{bat} is higher than its low level. Otherwise, the ultracapacitor supplies the demand if SOC_{UC} is higher than its low level. ii) Whenever the power demand is higher than the average power demand, both battery and UC share to meet the demand. iii) Whenever the required drive power demand is negative, which indicates braking, the ultracapacitor obtains that regenerative braking energy.

A 24 kWh battery was chosen for investigation. After scaling down by 10, a 2400 Wh battery was engaged. For the EUDC driving cycle, the peak power was estimated to be 16 kWh, so a 2 kW PMDC motor was selected. In addition, a 2000 Wh ultracapacitor was chosen, as its higher capacity can act as an energy buffer. Figure 6 shows the experimental setup.

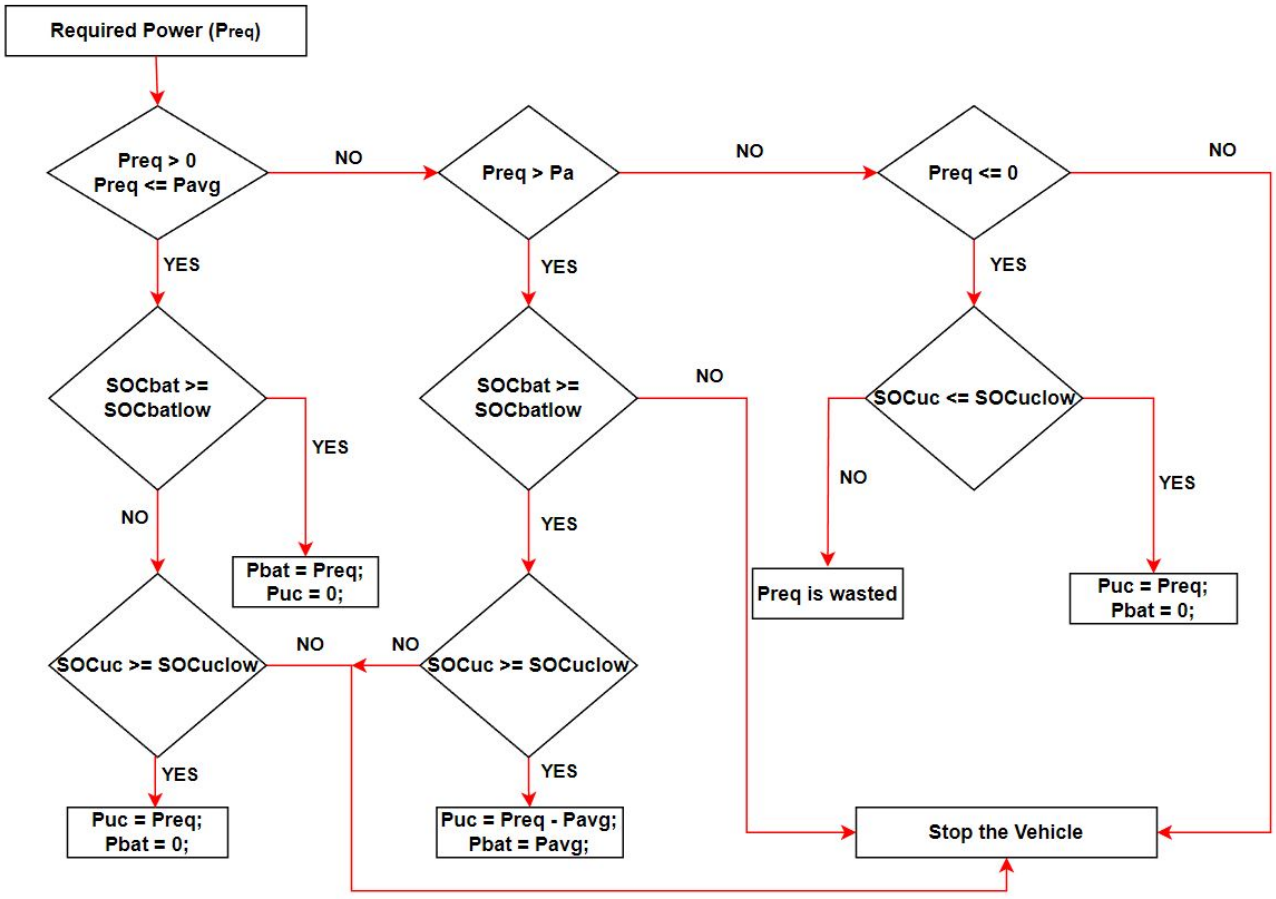

Figure 5. Rule-based control strategy.

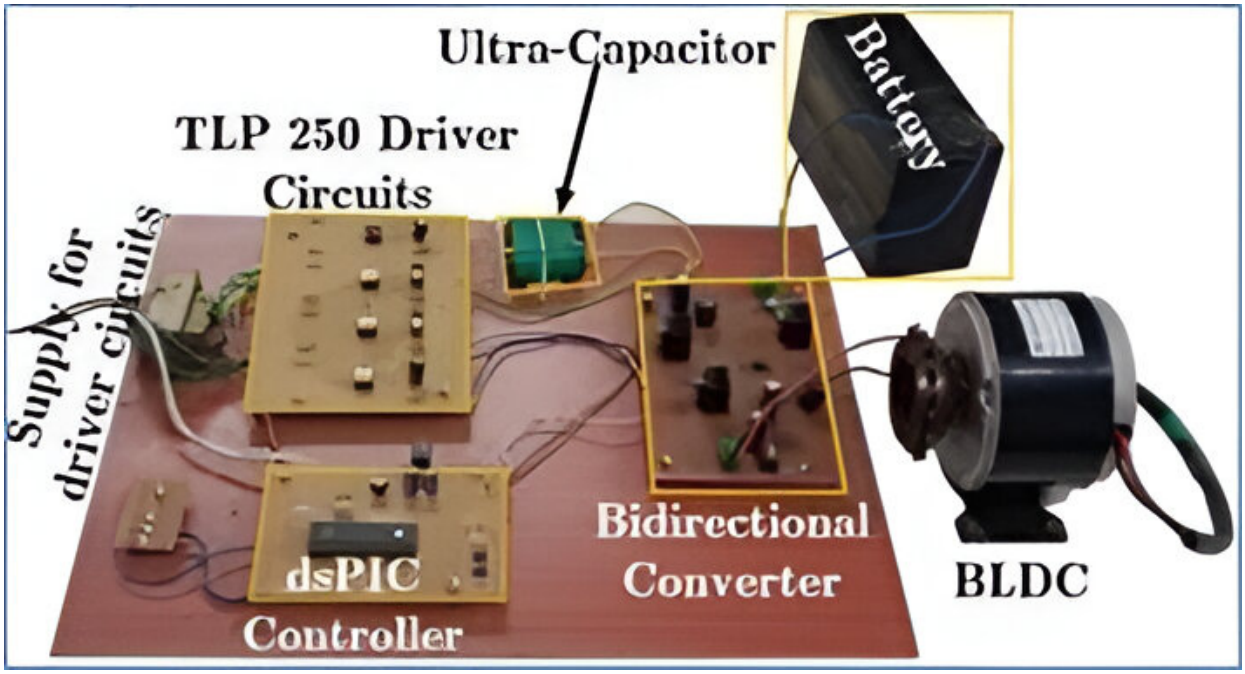

Figure 6. Experimental setup.

4. Results and discussion

The ANN model was first inspired by neuro-physics research that showed that the brain is made up of distinct cells called neurons that are connected to form networks. Every neuron has several dendrites (inputs), a soma (body), and an axon (output) that connect to the inputs of other neurons. Neurons function electrically, and we refer to such connections as synapses. Neurotransmitter fluid controls how synapses connect. The strengths and excitatory/inhibitory properties of the interconnections are determined by this fluid [28–30]. A neuron begins to fire an electrical signal to other neurons by axons when the total weighted inputs surpass a certain threshold value. When the weighted total of the neuron's inputs exceeds a certain threshold, the neuron is seen to fire. Frequent stimulation by incoming electrical pulses from linked axons of other neurons strengthens the weight of the synaptic connection. The following assumptions are made:

1. There must be synchronization among all neurons. This means that the time taken by each neuron to send an electrical signal to another neuron must be the same. Also, there must be synchronization in processing the signals for all neurons.
2. Each neuron owns a function called the activation function that decides the output electrical signal based on the strength of the input signal. That activation function must be independent of time.
3. As the electrical signals pass the synapse, the signals are reformed into a linear form, i.e., the electrical signal is a product of some controlling factor, the so-called synaptic weight.

A synaptic weight change concerning time is considered to be the most significant characteristic. This property ensures the possibility of the brain responding differently to the same input signal at different moments. The assumptions listed above simplify biological neural networks (NN). The distance between the neurons determines the time taken for the brain to transmit the signal naturally. Despite those assumptions, ANNs still offer the most significant properties of biological NN: flexibility and ability to learn.

ANNs comprise a single input layer (IL), some hidden layers (HL), and a single output layer (OL). Neurons are the building blocks of ANN. Synapses are the links between the neurons, and a weighting factor is allotted to each link. Thus, the weighting factor can be adjusted to obtain an optimized output. Several functions are generally utilized as activation functions, and it is not mandatory to apply the same activation function for all neurons present in a network. In many applications, activation functions are not linear. Some common activation functions are given in Table 2. This study focuses on the prediction of parameters in electric vehicles, which are highly nonlinear. Hence, the hyperbolic tangent type of activation function was selected.

Table 2. Activation functions.

S. No.	Equation	Range of values	Activation function
1.	$F(S) = kS, k \epsilon R$	$(-\infty, \infty)$	Linear
2.	$F(S) = \begin{cases} kS, S > 0, k \in R \\ 0, S \leq 0 \end{cases}$	$(0, \infty)$	Semi-linear
3.	$F(S) = \frac{1}{1 + e^{-aS}}$	(0, 1)	Sigmoid
4.	$F(S) = \frac{2}{1 + e^{-aS}} - 1$	(−1, 1)	Bipolar sigmoid
5.	$F(S) = \frac{e^{aS} - e^{-aS}}{e^{aS} + e^{-aS}}$	(−1, 1)	Hyperbolic tangent
6.	$F(S) = e^{-aS}$	$(0, \infty)$	Exponential
7.	$F(S) = \sin(S)$	(−1, 1)	Sinusoidal
8.	$F(S) = \frac{S}{a + \lvert S \rvert}$	(−1, 1)	Fractional
9.	$F(S) = \begin{cases} 1, S \geq 0 \\ 0, S < 0 \end{cases}$	(0, 1)	Step
10.	$F(S) = \begin{cases} 1, S \geq 0 \\ -1, S < 0 \end{cases}$	(−1, 1)	Signature
11.	$F(S) = \begin{cases} -1, S \leq -1 \\ S, -1 < S < 1 \\ 1, S \geq 1 \end{cases}$	(−1, 1)	Binary step

Multi-layer perceptron ANNs are feed-forward ANNs comprising several commonly interlinked layers of neurons. Those interlinked layers are fixed one after the other. Each neuron in each layer must be connected with all other neurons in other networks. The objective behind the design of multi-layer ANN is to solve more tedious issues. The unit step activation function is typically not appropriate for a multi-layer ANN. Instead, the sigmoidal transfer function is continuous and flexible. The most appropriate function must be nonlinear and differentiable at any point in time. Nonlinearity in the activation function is essential since the output required must be nonlinear. K ≥ 2 is the number of layers arranged as the perceptron. M denotes the number of networks. C is the group of neurons that divide into mutually equal subsets such as L_1, L_2 … L_K. The ANN layers are arranged layer by layer, IL is represented as L_1, HLs are represented as L_2, L_3, L_4,…L_{K-1}, and OL is denoted as L_K. The links are initially connected from IL neurons to all other neurons in HL1 through the weights. Similarly, each of the neurons in L_i is linked with all other neurons in L_{i+1}.

The ANN output of ANN is obtained in a sequential way, i.e., layer by layer. The activation functions and weights must be set by the ANN; hence, the output from each layer relies on the previous layer output. ANN training is referred to as tuning the ANN parameter, which is accomplished with a learning procedure. An adjustment is made in the weighting factor or bias of the ANN to obtain the desired system performance. In general, there are two types of learning models available for ANN: supervised learning ANN and unsupervised learning ANN. In supervised learning, the target that is expected to be attained for each of the input samples is well-known in advance, i.e., priority. A teacher is assumed to be present for providing the information. Therefore, it is termed as *supervised*. The training procedure continues until the error found between the expected and obtained values is minimal. On the other hand, in unsupervised learning, the target that is expected to be attained for each input sample is not known in advance. The weights are adjusted to obtain appropriate outputs. Both learning methods require some parts of the data to be used to train the model and others for testing. Throughout this work, a supervised method of learning is utilized. The training process of the ANN is further differentiated into offline and online learning. A complete dataset is employed to update the ANN weights in an offline learning scheme. Training occurs through a series of steps called epochs. The complete dataset is offered to the network during each epoch. Later, the error is found as the result of the epoch.

Each new sample is sensed, and weights are updated, in the case of online training. As weights are changed, the error is evaluated by calculating the differences between the present and past time values. Subsequently, the updates for the weights must be computed. This approximation is progressed iteratively. The incremental back propagation (IBaP) network updates its weights after presenting every pattern from the learning data set, as opposed to just after every iteration. The batch backpropagation (BBaP) network processes all learning data patterns, with weight updates occurring once every iteration. A heuristic adaptation of the backpropagation technique is called quick propagation (QuP), which is substantially quicker than conventional backpropagation. The step size of the Levenberg-Marquardt method is determined by a parameter that takes large values in the initial iterations and small values in subsequent stages. A number that lies between 0 and 1 is denoted as the learning rate. It decides the speed of the ANN to adjust itself toward the values given during the training period. This number may vary (increase or decrease) dynamically over time. A careful selection of this factor is required since values too small may lead to a slow learning process, while values too high may lead to divergence. The learning rate was set to 0.6, 0.3, 0.7, and 0.2 for BBaP, QuP, IBaP, and LMBaP, respectively.

The momentum indicates how the previous weights have affected the present one. It prevents the ANN from getting stuck with local minima. This factor must be carefully chosen from experimental knowledge. The momentum can be neglected; however, considering it may lead to a better performance. The momentum constant was set to 0.5, 0.8, 0.8, and 0.6 for BBaP, QuP, IBaP, and LMBaP, respectively. The NEURAL power software platform was used for creating and analyzing the ANN model.

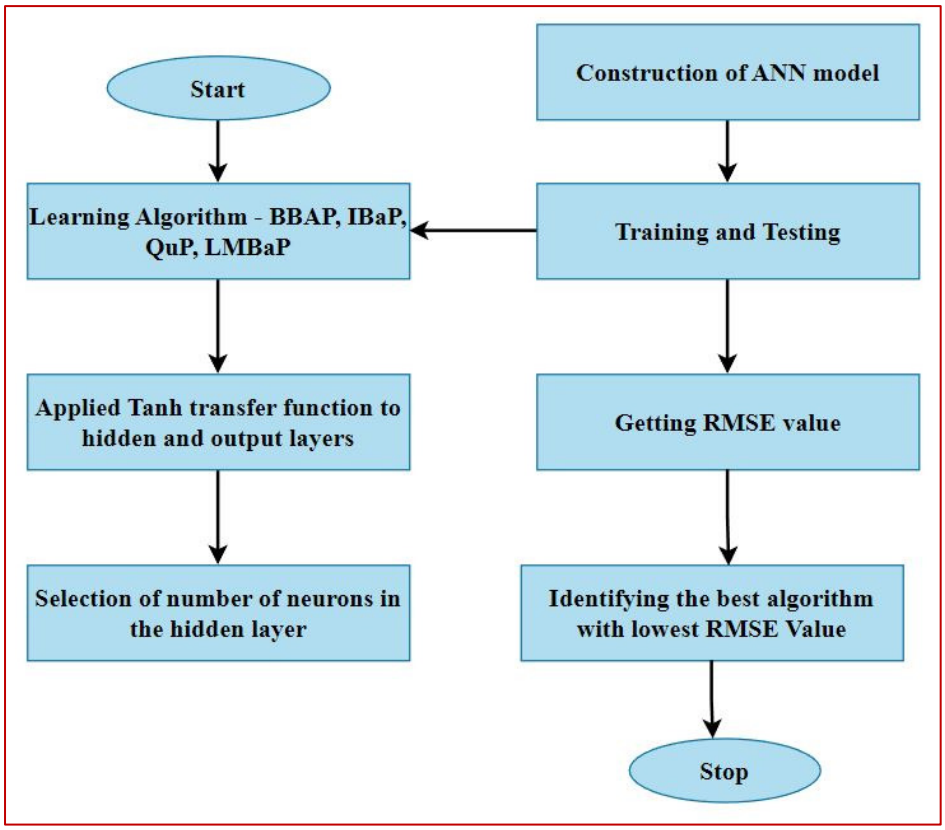

Figure 7. Logical flowchart of the ANN model for the prediction model.

Training and testing are the stages of ANN. During the training period, 75% of available data were utilized and the remaining 25% were allocated for testing the trained neurons in the prediction of output responses. Neurons' behaviors are controlled by different learning algorithms, transfer functions, and ANN architectures. The accuracy of the predicted data depends on the behavioral nature of the neurons. The quality of the prediction is determined by the RMSE value. The lower the RMSE value, the better the accuracy of the predicted value. The formula for calculating RMSE is given by Eq (7).

$$RMSE = \sqrt{\frac{1}{n}\sum_{i=1}^{n}(P-E)^2} \tag{7}$$

Here, E represents the experimental data, P denotes the predicted data, and n represents the number of testing data. The hyperbolic tanh function, as given in Eq (8), is selected for both the output and hidden layer.

$$f(x) = \frac{1-e^{-ax}}{1+e^{-ax}} \tag{8}$$

The flowchart of the ANN methodology is presented in Figure 7. The results obtained from L_9 OA experiments mentioned in Table 3 are used for training and testing the model.

Table 3. L_9 OA experimental results.

Experiment No.	Orthogonal array for control factors			Vehicle quality factors	
	VM	BS	UCS	ECR (Wh/km)	Battery stress (A)
1	A_1	B_1	C_1	13.09	4.88
2	A_1	B_2	C_2	13.31	4.94
3	A_1	B_3	C_3	12.3	4.67
4	A_2	B_1	C_2	12.77	4.84
5	A_2	B_2	C_3	12.41	4.70
6	A_2	B_3	C_1	14.27	5.09
7	A_3	B_1	C_3	12.89	4.83
8	A_3	B_2	C_2	14.53	5.17
9	A_3	B_3	C_1	14.44	5.15

Table 4. Characteristics of ANN.

Characteristics	Details
Training data	First 7 experiments
Testing data	8th and 9th experiments
Training algorithms	➢ Batch backpropagation (BBP) ➢ Quick propagation (QP) ➢ Incremental backpropagation (IBP) ➢ Levenberg–Marquardt backpropagation (LM)
Number of input neurons	3
Number of output neurons	2
Number of hidden layers	1
Number of neurons in the hidden layer	5–20
Number of iterations	1000

All 9 experiments were run with RBC, keeping vehicle mass, SOC_{BAT}, and SOC_{UC} as input control factors and ECR and battery stress as performance characteristics. During training, 75% of the data (i.e., the first 7 experiments) were selected, and the remaining 25% (8th and 9th experiments) were chosen for testing the designed ANN model. The characteristics of the ANN model chosen for the study are given in Table 4. Learning algorithms were selected based on their computational properties and the ability to work with nominal data. BBaP is stable for large sample data but converges more slowly. QuP has the advantage of faster convergence but has to be tuned appropriately because of stability issues. IBaP is best for updating data in real time. The LMBaP is less time-consuming but not very precise as compared with other methods; in this study, it proved to be the most effective method to minimize the RMSE in the small dataset. The performances of these algorithms were then thoroughly compared on different traffic-intensive types of vehicles. Four types of learning algorithms were chosen because of their computational capabilities and previous effectiveness in working with nonlinear data sets: batch backpropagation, quick propagation, incremental backpropagation, and Levenberg-Marquardt backpropagation. These algorithms were selected to compare the efficiency of the proposed method of minimizing the prediction error. LMBaP showed the lowest RMSE

value (0,06838). The learning rate and momentum constant for each algorithm were also optimized to avoid training instability. Here, the learning rate was 0.6 for BBaP and 0.3 for QuP. More specific details of the ANN architecture and the chosen algorithms point to the potential of the model for accurately estimating the operation of an HEV.

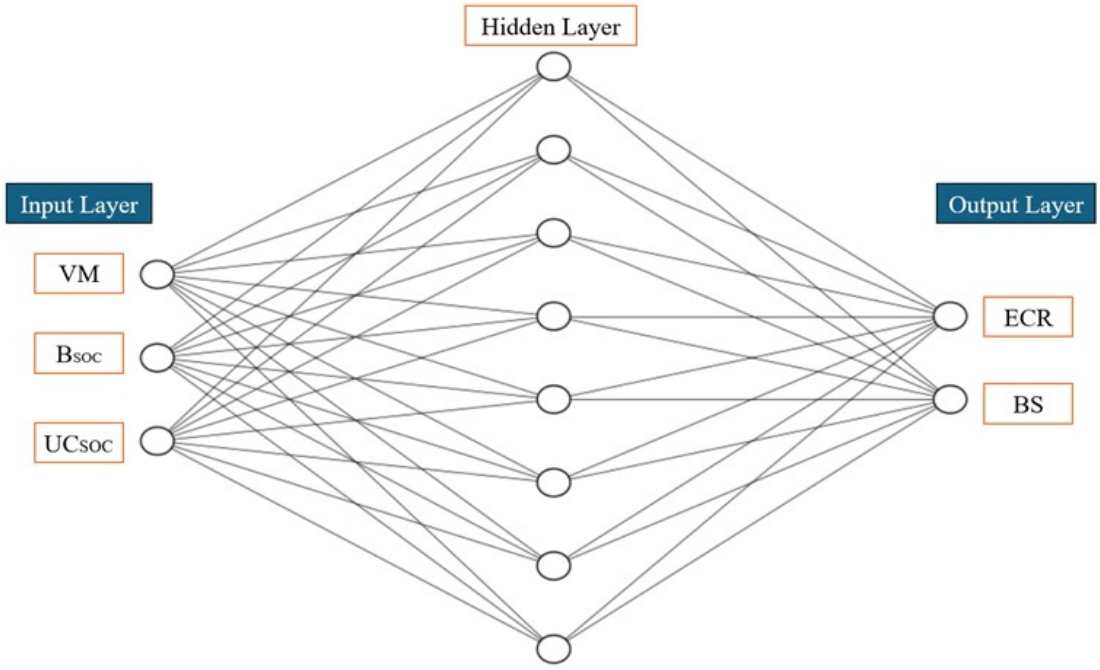

Figure 8. ANN structure for the prediction model.

As shown in Figure 8, the topology of an ANN network is made up of a single input layer that represents three control factors, a single hidden layer that contains eight neurons, and a single output layer that represents three output responses. Over a thousand repetitions were used to train each learning neuron. The neuron was trained using all four techniques, each of which has a different number of hidden layer neurons. Table 5 shows the average RMSE values obtained.

Table 5. Average RMSE values of the different learning algorithms.

Number of neurons in the hidden layer	Average RMSE			
	BBaP	IBaP	QuB	LMBaP
5	0.08193	0.09711	0.08190	0.069956
6	0.08781	0.09548	0.08558	0.07143
7	0.08771	0.09604	0.09064	0.07886
8	0.08071	0.09842	0.09138	0.06838
9	0.08584	0.09138	0.09125	0.07060
10	0.08178	0.09922	0.08277	0.07742
15	0.08408	0.09265	0.08235	0.07318
20	0.08417	0.09379	0.09081	0.06992

The LMBaP algorithm, with 8 hidden layer neurons, resulted in the lowest RMSE value of 0.06838. The trained and tested output data using the LMBaP algorithm are presented in Tables 6 and 7.

Table 6. Experimental values and training data for the LMBaP algorithm.

Experiment no.	ECR (Wh/km)			Battery stress (A/s)		
	Experimental	ANN	Difference	Experimental	ANN	Difference
1	13.09	13.53	0.44	4.88	4.75	0.13
2	13.31	13.86	0.55	4.94	5.05	0.11
3	12.30	12.25	0.05	4.67	4.72	0.05
4	12.77	13.27	0.50	4.84	5.01	0.17
5	12.41	12.67	0.26	4.70	4.81	0.11
6	14.27	14.60	0.33	5.09	4.76	0.33
7	12.89	12.72	0.17	4.83	4.75	0.08

Table 7. Experimental values and testing data for the LMBaP algorithm.

Experiment no	ECR (Wh/km)			Battery stress (A/s)		
	Experiment	ANN	Difference	Experiment	ANN	Difference
8	14.53	14.28	0.25	5.17	5.28	0.11
9	14.44	15.03	0.59	5.15	5.34	0.29

The experimental and predicted data for the performance characteristics were plotted to measure the accuracy of the prediction model.

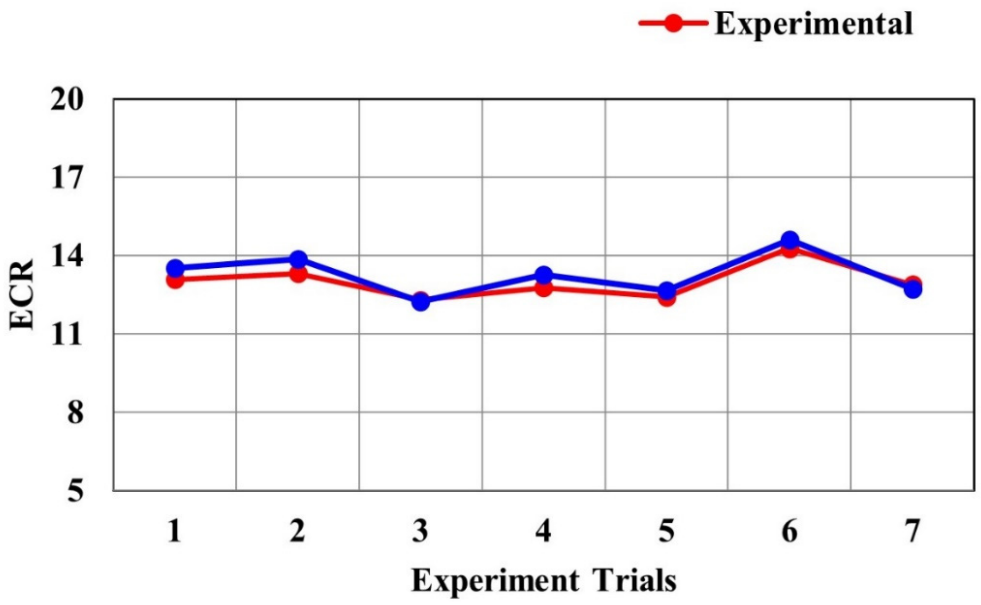

Figure 9. Predicted and experimental values for ECR.

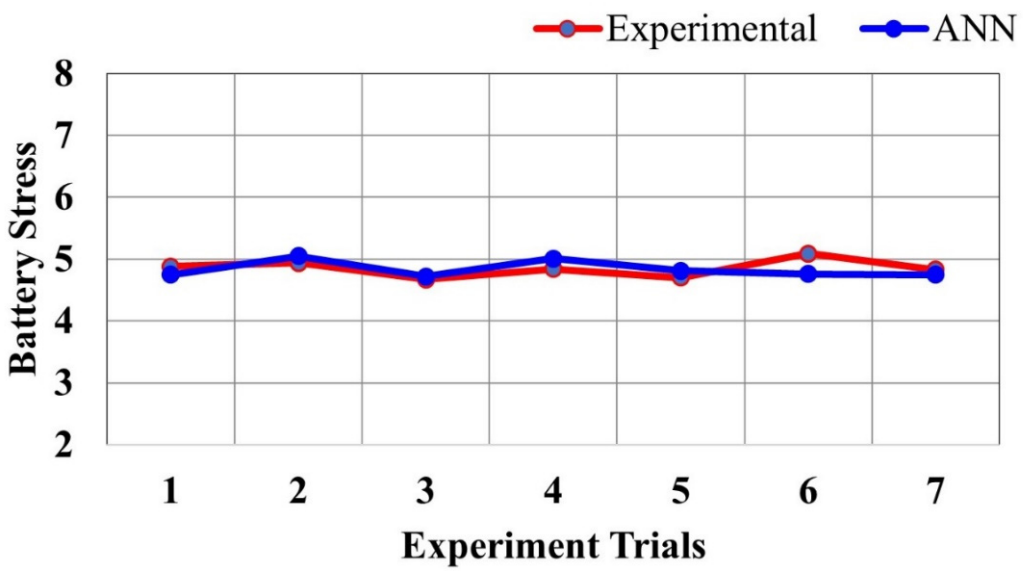

Figure 10. Predicted and experimental values for battery stress.

Figures 9 and 10 show the predicted and experimental values for ECR and battery stress, respectively. The differences between experimental and predicted data are almost negligible, which indicates that the prediction ANN model is accurate for the vehicle system considered.

Also, the computation time of each algorithm was calculated. LMBaP offered the best tradeoff between accuracy and time. These results were obtained after trying the algorithms under different configurations of hidden layers, which also confirmed that LMBaP maintained lower error rates in comparison to others. Variability in input control factors and lack of finer gradients of driving cycle data were also considered to identify possible sources of error. Slight discrepancies between experimental and predicted values uphold the efficiency of the ANN model in predicting the performance of the vehicle. These results are crucial to enable the best energy control methodologies for HEVs, more so under realistic traffic scenarios. The convergence graph of one sample run of the training is provided in Figure 11. The corresponding original and cumulative weight statistics are shown in Figure 12. The results of the sensitivity analysis indicate that LMBaP outperformed other algorithms, especially under dynamic traffic conditions, with a 10% and 15% reduction in RMSE compared with QuP and BBaP, respectively. However, QuP's faster convergence proved to be important for simpler, uniform driving cycles. Realistic driving data shows inherent variability and, due to modeling assumptions and physical limitations, input parameters have limited granularity. This explains the discrepancies between experimental and predicted values. Errors from these extrapolations can be minimized by future studies that use finer data resolution.

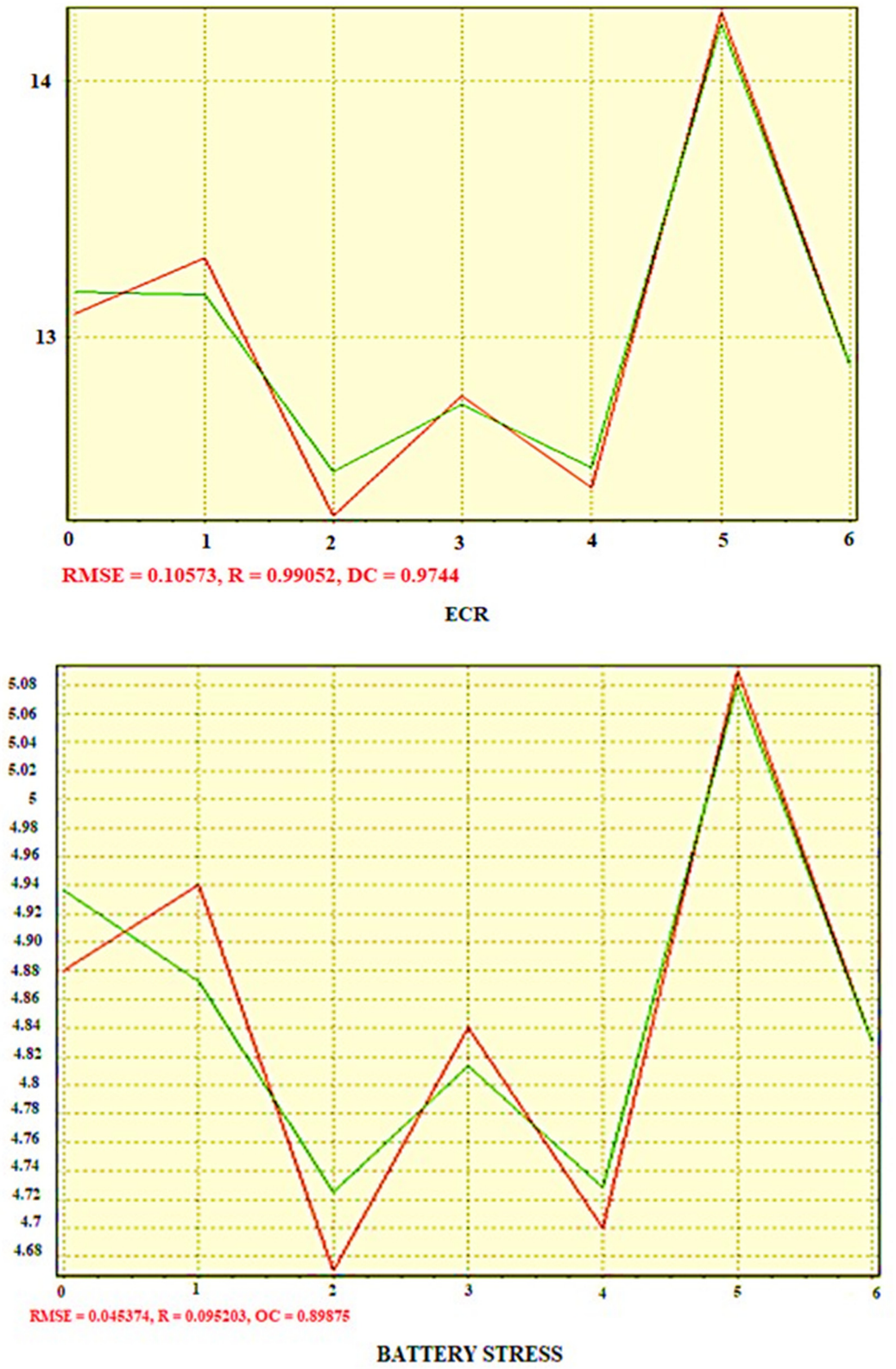

Figure 11. Convergence graph of ECR and battery stress.

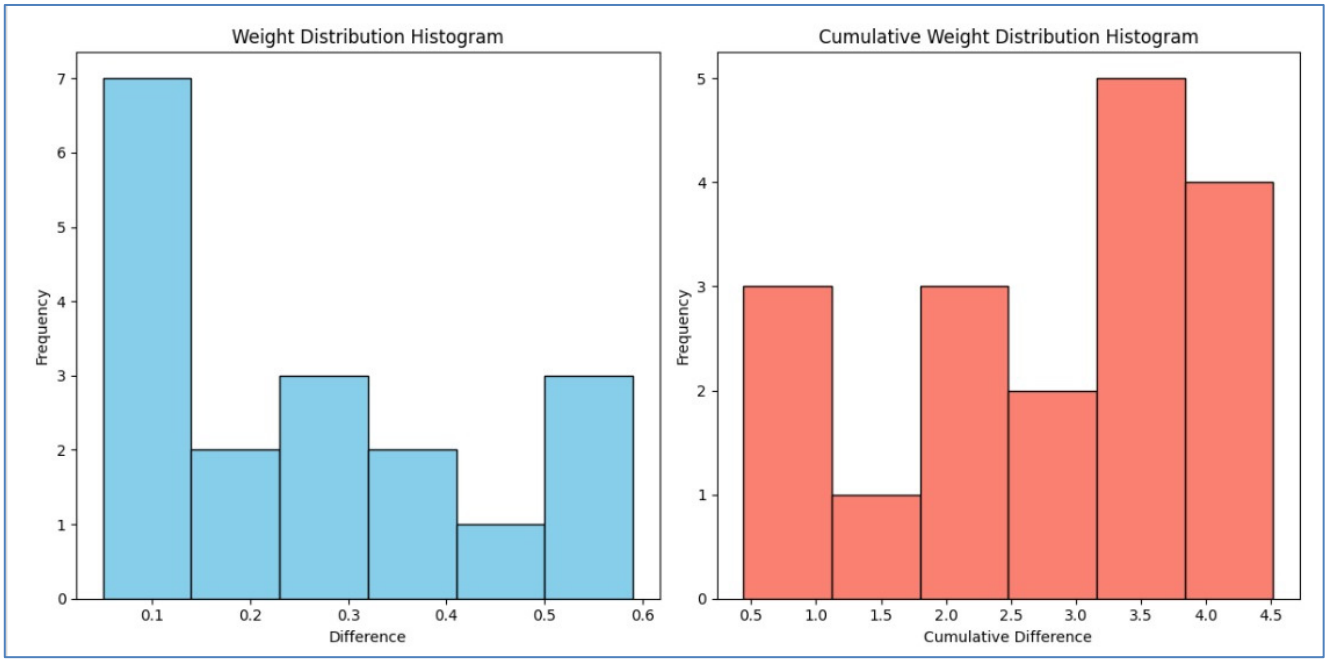

Figure 12. Weight statistics are original and cumulative.

5. Conclusions

In this study, an ANN model was established to provide the energy consumption rate (ECR) and battery stress of HEVs based on the correlation between performance control factors and vehicle performance. The following conclusions can be drawn:

(1) To integrate the ECR and battery stress analysis of HEVs, an artificial neural network (ANN) model was designed to predict the energy consumption rate (ECR). The experimental dataset was split into a training data set (75%) and a testing data set (25%).

(2) Different learning algorithms, such as batch backpropagation (BBaP), quick propagation (QuP), incremental backpropagation (IBaP), and Levenberg–Marquardt backpropagation (LMBaP), were used; the lowest RMSE (0.06838) was achieved by the LMBaP algorithm, with 8 hidden layer neurons.

(3) Good correlations between ANN predictions and experimental values demonstrated the adequacy of the model in predicting both ECR and battery stress for enhancing the performance of vehicles under different control factors.

(4) The insights derived from the model assist in properly locating charging stations, managing the vehicle scheduling for efficient use, and preventing waste of energy in the development of EV charging stations.

(5) The proposed method has the potential to facilitate green mobility planning because it optimizes energy consumption and decreases GHG emissions and battery stress while increasing battery cycle length and decreasing the battery replacement frequency.

The predicted values can inform the location of charging spots and the alteration of the car schedules to mitigate energy loss and complement infrastructure development and green mobility planning. Prediction measures can be further improved by including dynamic traffic condition data, natural conditions, and vehicle data. However, the application of less conventional algorithms in

machine learning approaches such as reinforcement learning can enhance the flexibility of energy management solutions. A thorough consideration of how to design the network of multi-vehicles and the placement of charging stations can assist with obtaining widespread EV acceptance.

Use of AI tools declaration

The authors declare they have not used Artificial Intelligence (AI) tools in the creation of this article.

Conflict of interest

The authors declare no conflict of interest.

Author contributions

A.Geetha: Conceptualization, Resources, Data curation, Writing original draft; S.Usha: Software, Validation, Methodology, Writing review, editing; J. Santhakumar: Investigation, Visualization, Data curation, Software; Surender Reddy Salkuti: Methodology, Formal analysis, Project administration, Supervision, Writing—review and editing.

Acknowledgments

This research work was supported by "Woosong University's Academic Research Funding-2025".

References

1. Moreno J, Ortuzar ME, Dixon JW (2006) Energy-management system for a hybrid electric vehicle, using ultracapacitors and neural networks. *IEEE Trans Ind Electron* 53: 614–623. https://doi.org/10.1109/TIE.2006.870880
2. Hideki K, Ryosuke A, Yoshinori K, et al. (2016) The eco-driving effect of electric vehicles compared to conventional gasoline vehicles. *AIMS Energy* 4: 804–816. https://doi.org/10.3934/energy.2016.6.804
3. Sun S, Li T (2024) An analysis of the global EV market: Sustainable pathways to net zero emissions. *J Appl Econ Policy Stud* 11: 67–80. https://doi.org/10.54254/2977-5701/11/2024104
4. Dalong G, Chi Z (2016) Potential performance analysis and future trend prediction of electric vehicle with V2G/V2H/V2B capability. *AIMS Energy* 4: 331–346. https://doi.org/10.3934/energy.2016.2.331
5. Zhang S, Xiong R (2015) Adaptive energy management of a plug-in hybrid electric vehicle based on driving pattern recognition and dynamic programming. *Appl Energy* 155: 68–78. https://doi.org/10.1016/j.apenergy.2015.06.003
6. Samson OS, Atanda KR (2022) State-of-the-art review of fuel cell hybrid electric vehicle energy management systems. *AIMS Energy* 10: 458–485. https://doi.org/10.3934/energy.2022023
7. Kraa O, Ghodbane H, Saadi R, et al. (2015) Energy management of fuel cell/supercapacitor hybrid source based on linear and sliding mode control. *Energy Proc* 74: 1258–1264. https://doi.org/10.1016/j.egypro.2015.07.770

8. Eduardo EMJ, António MNQ, Santos DMF (2023) Economic analysis of lithium-ion battery recycling. *AIMS Energy* 11: 960–973. https://doi.org/10.3934/energy.2023045
9. Attanayaka AMSMHS, Karunadasa JP, Hemapala KTMU (2019) Estimation of state of charge for lithium-ion batteries—A review. *AIMS Energy* 7: 186–210. https://doi.org/10.3934/energy.2019.2.186.
10. Steven BS, Zachary PC, Michael F, et al. (2018) Range-extending zinc-air battery for electric vehicle. *AIMS Energy* 6: 121–145. https://doi.org/10.3934/energy.2018.1.121
11. Kritanjali D, Santanu S (2022) Coulombic efficiency estimation technique for eco-routing in electric vehicles. *AIMS Energy* 10: 356–374. https://doi.org/10.3934/energy.2022019
12. Caroline B, Stéphane R, Melika H, et al. (2021) Direct fuel cell—Supercapacitor hybrid power source for personal suburban transport. *AIMS Energy* 9: 1274–1298. https://doi.org/10.3934/energy.2021059.
13. Geetha A, Subramani C (2017) A comprehensive review on energy management strategies of hybrid energy storage system for electric vehicles. *Int J Energy Res* 41: 1817–1835. https://doi.org/10.1002/er.3730
14. Ruchen H, Hongwen H, Xuyang Z, et. al. (2022) Battery health-aware and naturalistic data-driven energy management for hybrid electric bus based on TD3 deep reinforcement learning algorithm. *Appl Energy* 321: 119353. https://doi.org/10.1016/j.apenergy.2022.119353
15. Huang R, He H, Su Q (2024) Towards a fossil-free urban transport system: An intelligent cross-type transferable energy management framework based on deep transfer reinforcement learning. *Appl Energy* 363: 123080. https://doi.org/10.1016/j.apenergy.2024.123080
16. Berjoza D, Jurgena I (2017) Effects of change in the weight of electric vehicles on their performance characteristics. *Agron Res* 15: 952–963. Available from: https://agronomy.emu.ee/wp-content/uploads/2017/04/Vol15SP1_Berjoza.pdf.
17. Wang R, Shi X, Su Y, et. al. (2024) A predictive energy management strategy for plug-in hybrid electric vehicles using real-time traffic based reference SOC planning. *Proc Inst Mech Eng Part D* 1: 1–10. https://doi.org/10.1177/09544070241239996
18. Abdelrahman K, Samir K, Taher E (2023) Prediction of the equivalent circulation density using machine learning algorithms based on real-time data. *AIMS Energy* 11: 425–453. https://doi.org/10.3934/energy.2023023
19. Xiaoyu Z, Dewang C, Yusheng W, et al. (2023) Remaining useful life indirect prediction of lithium-ion batteries using CNN-BiGRU fusion model and TPE optimization. *AIMS Energy* 11: 896–917. https://doi.org/10.3934/energy.2023043
20. Linda G, Roy C (2002) Operation of an aluminum-intensive vehicle: Report on a six-year project. *Cent Transp Res Argonne Natl Lab* 1: 1–9. https://doi.org/10.4271/2002-01-2066
21. Martin M, Igor GLK, Dalibor B (2016) Analysis of parameters influencing electric vehicle range. *Proc Eng* 134: 165–174. https://doi.org/10.1109/TII.2015.2404800
22. Yang C, Du X, Wang W, et al. (2024) Variable optimization domain-based cooperative energy management strategy for connected plug-in hybrid electric vehicles. *Energy* 15: 1–17. https://doi.org/10.3390/wevj15080350
23. Rauh N, Franke T, Krems JF (2015) User experience with electric vehicles while driving in a critical range situation—A qualitative approach. *IET Intell Transp Syst* 9: 734–739. https://doi.org/10.1049/iet-its.2014.0214

24. Huang R, He H, Zhao X, et al. (2023) Longevity-aware energy management for fuel cell hybrid electric bus based on a novel proximal policy optimization deep reinforcement learning framework. *J Power Sources* 561: 232717. https://doi.org/10.1016/j.jpowsour.2023.232717
25. Shuo Z, Rui X, Xuan Z (2015) Comparison of the topologies for a hybrid energy-storage system of electric vehicles via a novel optimization method. *Sci China Technol Sci* 58: 1173–1185. http://doi.org/10.1007/s11431-015-5843-y
26. Qusay H, Sameer A, Aws ZS, Hayder MS, et al. (2023) A review of hybrid renewable energy systems: Solar and wind-powered solutions: Challenges, opportunities, and policy implications. *Results Eng* 20: 101621. https://doi.org/10.1016/j.rineng.2023.101621
27. Staackmann M, Liaw BY, Yun DYY (1997) Dynamic driving cycle analyses using electric vehicle time-series data. *IEEE Int Electr Veh Conf Proc* 1: 2014–2018. http://doi.org/10.1109/IECEC.1997.656736.
28. Momenimovahed A (2014) Real-time driving cycle measurements of ultrafine particle emissions from two wheelers and comparison with passenger cars. *Int J Automot Technol* 15: 1053−1061. http://doi.org/10.1007/s12239−014−0109−4
29. Zhihan L, Wenlong S (2023) Impacts of intelligent transportation systems on energy conservation and emission reduction of transport systems: A comprehensive review. *Green Technol Sustainability* 1: 100002. https://doi.org/10.1016/j.grets.2022.100002
30. Vishal P, Varshaben S (2015) Measurement and analysis of Indian road drive cycles for efficient and economic design of HEV component. *World Electr Veh J* 7: 1–12. https://doi.org/10.3390/wevj7010121